Topics in Catalysis
https://doi.org/10.1007/s11244-019-01199-6

ORIGINAL PAPER

Adsorption and Decomposition of Glycerol on Pristine and Oxygen Modified Au(111) Surfaces

Florencia C. Calaza[1] · **Miguel A. Baltanás**[1] · **Martin Sterrer**[2] · **Hans-Joachim Freund**[3]

Abstract

Research on biomass derived raw materials for conventional catalytic processes, especially those directed to replace human dependence on fossil-based energy, is a high priority academic topic worldwide. Glycerol, the ubiquitous by-product of biodiesel manufacture, is seen as a promising building block due to its versatile functionality. Hence, research efforts to valorize it by selective partial oxidation are widespread. Fundamental knowledge of the interaction of glycerol with metal surfaces in the presence of oxygen is of extreme importance to rationally design new catalytic materials. In this work, a complete study of glycerol interaction with pristine and oxygen modified Au(111) surfaces is presented, by means of X-ray photoelectron and infrared reflection absorption spectroscopies, aided by temperature programmed desorption (TPD) experiments using mass spectrometry. On the clean Au(111) surface, glycerol adsorbs at 150 K through weak interactions between the oxygen atoms from OH groups and gold atoms. No thermal activation is observed and only molecular desorption is detected in TPD at 293 K. On the other hand, when the Au surface is precovered with oxygen atoms in the form of chemisorbed oxygen, glycerol adsorbs in a slightly different geometry and is activated even at low temperatures. The observation of spectral features related to C=O bonds clearly corroborates the activation of the alcohol groups toward partial oxidation intermediates. Possible products desorbing from the surface due to this activation are identified as dihydroxyacetone, hydroxypiruvic, tartronic and formic acid, as well as H_2O and CO_2.

Keywords Glycerol · Gold · Adsorption · XPS · IRAS · TPD

1 Introduction

Even though industrial societies worldwide still depend on fossil resources to produce the majority of fuels and important commodity chemicals demanded by their economies, growing environmental concerns have boosted basic and applied research efforts towards the use of biomass as an urgently needed, more eco-friendly substitute [1–4]. In this regard, lignocellulose-based materials are the preferred feedstock, because of its non-edible nature [2, 4, 5]. Nonetheless, the economic realization of large scale biorefineries able to produce just the desired chemicals still confronts many hurdles, among which is the capability to find a market for the large amount of byproducts generated by the available, state-of-the-art technology. In the meantime first generation biofuels, such as the biodiesel produced mostly from soybean, rapeseed and palm oil, stand out as the only available substitute to fossil fuels able to contribute—so far—to slowing down global warming [6, 7].

Biodiesel manufacturing, in turn, generates crude glycerol as byproduct (approx. 10% of the biodiesel tonnage), which urgently needs to be transformed into more valuable chemicals because the constant, yearly increase in biodiesel production has led to a high surplus of said chemical (as well as a drastic drop of its price) [8]. Fortunately, substantial effort has already, and is constantly, been put into the development of new technologies and catalytic routes for its

---

Electronic supplementary material The online version of this article (https://doi.org/10.1007/s11244-019-01199-6) contains supplementary material, which is available to authorized users.

✉ Florencia C. Calaza
fcalaza@intec.unl.edu.ar

[1] Instituto de Desarrollo Tecnológico para la Industria Química (INTEC), UNL-CONICET, Güemes 3450, 3000 Santa Fe, Argentina

[2] Institute of Physics, University of Graz, NAWI Graz, Universitätsplatz 5, 8010 Graz, Austria

[3] Fritz-Haber-Institut der MPG, Faradayweg 4-6, 14195 Berlin, Germany

conversion into more value-added products [8–11], where selective oxidation routes appear as the most promising ones [12, 13]. Precious metals have been singled out as the preferred choice to realize the multiple goals of catalytic activity, selectivity and durability, among which the performance of gold (pure or alloyed), particularly at low-temperature process conditions, has been found truly outstanding [14–20].

Yet, despite the enormous progress of catalysis science both at the theoretical and experimental level [17–28], in depth understanding of the pathways of these reactions at the molecular scale is still elusive, and continuous effort is being put into the generation of a robust data base from which effective R&D actions can be undertaken. Thus, modeling of adsorption/reaction processes by means of surface-science techniques using single crystal surfaces and model adsorbates has become a persuasive approach to help in the quest for a more rational design of active, selective and competitive (viz., durable) catalysts for glycerol valorization via partial oxidation. This paper, then, presents an experimental study of the interaction of glycerol with clean and modified Au(111) surfaces, aiming to present new evidence about the pathway of glycerol activation on the surface of Au.

Adsorption of alcohol molecules on coinage metals has been studied in the past. Methanol adsorbs on the low Miller-index surfaces of gold, silver and copper in molecular form [29–37]. The cleavage of the O–H bond to form methoxy species adsorbed is only achieved in the presence of chemisorbed oxygen [34–36] or on stepped surfaces, like Au(310) [37]. These findings are in contrast to those for adsorption of methanol on more reactive metals like Pt [38, 39] or Pd [40, 41], where the stronger interaction leads to OH bond cleavage and the formation of methoxy species beside molecular adsorption at low temperature. It was shown experimentally that for all cases the alcohol molecule interacts directly with the surface through the electron lone pair of the oxygen atom in OH, providing the necessary closeness for breaking the O–H bond for the more reactive metallic surfaces. Experimental research of diols adsorption on metallic and metal oxide surfaces [32, 42–49] has received some interest in the past, especially for interaction of ethylene glycol and 1,2- or 1,3-propanediol as model compounds of biomass related catalytic processes. On all surfaces where comparison could be made, the adsorption of diols is stronger than that of monoalcohol molecules. This is due not only to the higher molecular weight of the former, but also to the presence of a second OH group imposing a second point of interaction between the molecule and the surface, thus implying that the position of the OH groups and their distance from each other will definitely dictate the chemistry seen. There is no work on diols adsorption on gold single crystals and the closest metal, in terms of reactivity, to compare with is copper, e.g.,by looking at the work by Bowker and Madix [32] on adsorption and reactivity of several alcohols, including ethylene glycol, on Cu(110). It was found the diol adsorbs more strongly than any of the other C1–C4 monoalcohols studied, and through the OH groups, by dissociating both of them to form a dialcoxy, which further dehydrogenates to liberate mostly glyoxal upon heating. For comparison with a trialcohol, or glycerol, which is the object of study of this work, there is no spectroscopy data available from its interaction with any single crystal surface. To the best of our knowledge, only one published work by Skoplyak et al. [50] studied the adsorption and further decomposition of glycerol on model bimetallic surfaces of Ni–Pt–Pt(111) by means of TPD experiments, showing enhanced production of H_2 when a monolayer of Ni atoms is exposed on the surface.

Herein, we have used XPS, IRAS and TPD to follow the adsorption behavior and decomposition pathway of glycerol on Au surfaces.We find that while molecular adsorption of glycerol prevails on clean Au(111), the reactivity is enhanced on oxygen-precovered Au(111), providing a pathway for the partial oxidation of glycerol.

2 Experimental Details

The experiments were performed within a single ultra-high vacuum system operating at a base pressure of 1×10^{-10} mbar and consisting of a preparation/analysis chamber equipped with standard tools for single-crystal preparation, a low-energy electron diffraction (LEED) unit, a quadrupole mass spectrometer for temperature programmed desorption (TPD) experiments, and a dual-anode X-ray source and a hemispherical electron analyzer for X-ray photoelectron spectroscopy (XPS). An UHV-elevated pressure cell connected to the bottom of the main UHV chamber, which is equipped with CaF_2 windows for optical access of the sample to infrared radiation, allows to record in situ infrared reflection absorption (IRA) spectra up to 1 bar total pressure. The single-crystal sample was mounted on a manipulator, which allowed transferring the sample between the preparation chamber and the elevated pressure cell. The samples could be heated in UHV up to 1400 K via resistive heating, or cooled to 90 K using liquid nitrogen.

The disc-shaped Au(111) sample (10 mm diameter) was directly mounted on the manipulator via Ta wires, and the temperature was monitored with a type-K thermocouple. The Au(111) surface was cleaned by cycles of sputtering (Ar^+, 1 keV, 30 min) and annealing. Typically, after sputtering the sample at room temperature, it was first annealed for 5 min at 900 K and then cooled to 600 K, at which it was tempered for an additional 30 min. This procedure was repeated until sharp LEED spots of the Au(111) $22 \times \sqrt{3}$ herringbone reconstruction were obtained [51–53].

XPS was used to check the cleanliness of the sample and to study adsorbed species after adsorption of glycerol and/or oxygen. XP spectra were acquired at an electron takeoff angle of 60° relative to the surface normal and with a pass energy of 20 eV.

For the formation of chemisorbed oxygen atoms, the Au(111) sample surface was positioned in front (~ 2 cm away) of a glowing tungsten filament while backfilling the chamber with O_2 (1×10^{-7} mbar). A calibration of the amount of oxygen chemisorbed on Au(111) was obtained by following the O1s and Au4f signal evolution with XPS with increasing time of oxygen exposure (see Supporting Information).

The IRAS measurements were performed using a Bruker IFS66v Fourier-transform infrared spectrometer with an external, LN_2-cooled mercury–cadmium–telluride detector. Typically, 1000 scans were averaged for one spectrum with the resolution set to 4 cm^{-1}. The IRA spectrum of a clean Au(111) surface was used for background correction, unless otherwise stated. The heating rate during TPD runs was 1 K/s.

Glycerol (Sigma Aldrich, ≥ 99.5%) was dosed by evaporation of the liquid from a vial via a leak valve connected directly to an IR cell port facing the sample. Furthermore, the leak valve was modified by addition of a stainless steel tube (distance from end of tube to sample surface: 1 in; diameter 1/4 in). To obtain a reasonable deposition rate of glycerol, the glass vial was submerged into a (water + glycerol) bath maintained at a temperature of about 370 K. The gas line and the leak valve (stainless steel) were also heated to approximately 355 K to minimize condensation of glycerol inside. Glycerol has a very low vapor pressure (0.0002 mmHg @ 25 °C), is viscous in nature and working with it is not a trivial task, if one wants to perform clean dosing. The doses presented here were calibrated as Langmuirs ($1\ L = 1 \times 10^{-6}$ Torr s) by monitoring the change in background pressure of the IR cell. Calibration might be off by about a factor of 5 (comparing with similar compounds) or more due to the pressure reading not being corrected for ion gauge sensitivity gauge. Therefore, it needs to be stressed that all doses presented here are merely orientative of the time the sample is exposed to glycerol before the respective measurement.

3 Results and Discussion

3.1 Adsorption of Glycerol on Clean Au(111)

The adsorption of glycerol (Gly) was performed directly on the IRAS UHV-HP cell; the corresponding IRA spectra during adsorption and for all increasing exposures were acquired while holding the sample temperature at 150 K. After exposure to a given amount of glycerol the sample was transferred to the UHV preparation chamber where XPS and TPD measurements were performed, obtaining in this way a calibration curve for the respective signals versus exposure. The results from these experiments are shown in Fig. 1a–c, where the XP spectra for the regions O1s, C1s and Au4f are depicted.

In the O1s region (Fig. 1a), a signal centered at 532.3 eV appears right upon adsorption and is still observed at the same binding energy upon exposure to 100 L. The signal for C1s related to HO–**C**H_x carbon type is observed at 285.9 eV (Fig. 1b), for doses up to 100 L. The binding energies of these signals are characteristic of intact C–O–H bonds from alcohol molecules adsorbed on surfaces, thus correspondingly assigned here to the three alcohol moieties of glycerol. With the analyzer resolution used, distinction between primary and secondary alcohols could not be attained, neither for O1s nor for C1s. In Fig. 1c, the corresponding XP spectra for the Au4f region are plotted, showing the Au $4f_{7/2}/4f_{5/2}$ doublet at 84.0 and 87.6 eV, respectively. From the first dose of glycerol and for all continuing doses, the Au4f signal shifts by 0.1 eV toward higher binding energies. No other shifts were observed at higher glycerol exposures, whereas a decrease in the Au4f signal intensity could be correlated with the increasing coverage of glycerol, up to the formation of multilayers. Note that the C1s and O1s signals shift to higher binding energies with increasing glycerol exposure, reaching 286.5 and 532.8 eV at exposures of 500 L, respectively.

A plot of the integrated XP peak areas obtained from the spectra presented in Fig. 1a, b (C1s and O1s) versus glycerol dose is shown in Fig. 2. These results suggest that a full monolayer of glycerol is obtained for doses between 50 and 100 L. An exact value cannot be established because of the weak nature of glycerol adsorption on Au, which makes it difficult to distinguish a breaking point beyond which second and multilayers start growing. This effect is not uncommon for molecular adsorption on any of the coinage metals [31–37]. Besides, probably the formation of adsorbate islands occludes differentiation between mono and successive layers. Yet, one possible clue for stating at which point second layers start growing can be inferred from the shift in the peak positions of either C1s or O1s XP signals, and these are plotted in Fig. 2 on the right axis. Both signals are observed to be centered at the same binding energy (285.9 eV for C1s and 532.3 eV for O1s) until the same range of glycerol exposure (50 to 100 L) is reached, and increase steadily afterwards, showing a typical behavior for growing layers which are not in direct contact with the surface.

A set of IRA spectra showing the vibrational features corresponding to glycerol adsorbed on the Au surface, growing with increasing doses, is plotted in Fig. 3. At the smallest

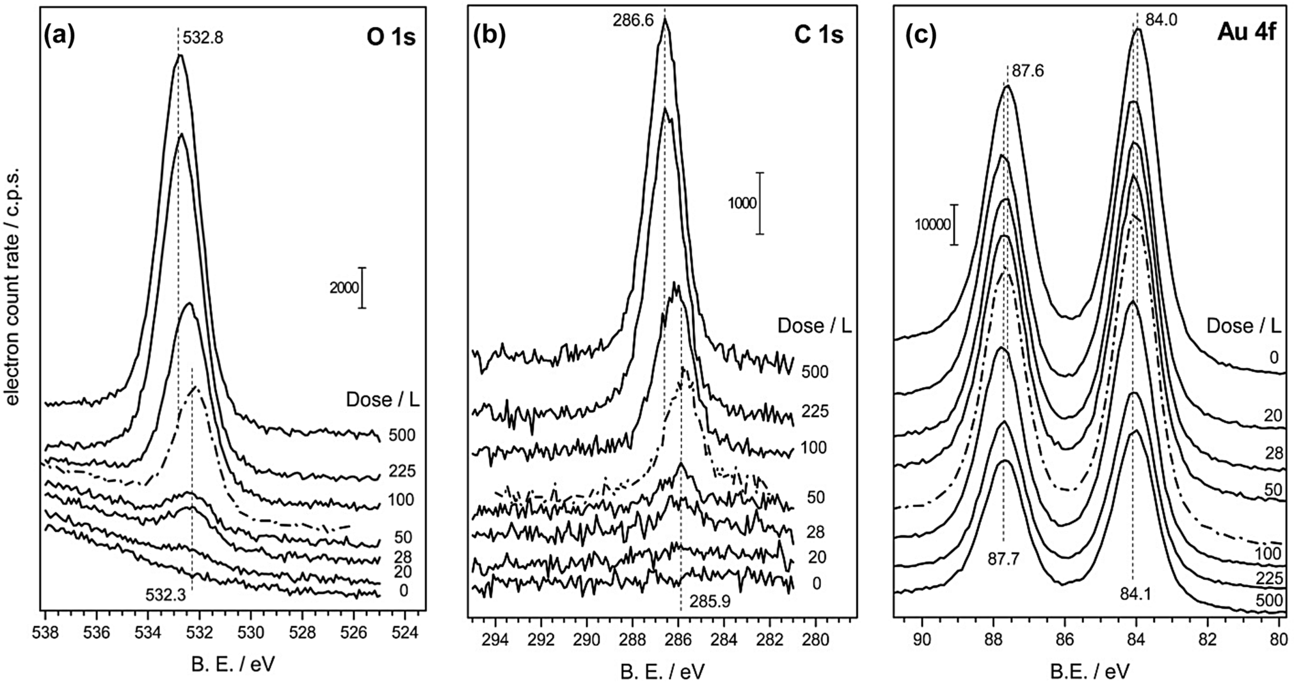

Fig. 1 XP spectra at increasing doses of glycerol (in Langmuirs) on Au(111) at 150 K. **a** O1s, **b** C1s and **c** Au4f regions. The dashed line between the 50 and 100 L doses correspond to a 120 L glycerol exposure at 150 K, further annealed to 260 K. All XP spectra were recorded at 150 K

dose (20 L), a few features are already visible, at 3440, 2880–2935, 1322 and 1115 cm^{-1}. They correspond to some of the characteristic vibrations of glycerol and continue to increase in intensity with increasing doses. The broad feature at 3440 cm^{-1} that presents a tail on the lower wavenumber side corresponds to the hydroxyl stretches (υOH), most probably exhibiting some degree of intra or intermolecular hydrogen bonding. By the second dose (30 L), the tail starts growing and it fully develops as a peak at 3320 cm^{-1} after the 90 L dose. By this exposure, another peak at 1460 cm^{-1} clearly shows up, which corresponds to the symmetric CH_2 bending (δ_sCH_2). In the CH stretching region, two bands are observed already at low doses, at 2880 and 2933 cm^{-1}, which are assigned to the asymmetric and symmetric CH_2 stretching modes of glycerol molecules, respectively. These two bands are the most prominent in this region, but they are accompanied by shoulders at 2844 and 2955 cm^{-1}, even though the latter are not easy to discern when multilayers start growing and all the bands in the region become broader. The CH and CH_2 bending modes are observed at 1400–1460 and 1336 cm^{-1}, and grow in parallel with the stretching modes. Lastly, in the low wavenumber region two vibrations are clearly observed at 1120 and 1060 cm^{-1}, especially when multilayers are formed. They correspond to the C–O stretching modes of the alcohol moieties, as per the following assignment: the one at 1120 cm^{-1} is the primary (terminal) and the one at 1060 cm^{-1} is the secondary (central) C–OH group. At doses corresponding to multilayer formation (100 to 500 L), all observed vibrational bands are in full agreement with the IR spectrum of liquid glycerol (NIST spectrum [54]). All vibrational assignments of bands observed in Fig. 3 are summarized in Table 1, together with available literature of glycerol IR studies for comparison.

When analyzing results from IRA spectra, it needs to be remembered that the non-observation of signals does not imply their non-existence. Due to surface selection rules, a certain molecular vibration might not be visible simply because it has no component of the change in dipole moment aligned with the surface normal (perpendicular to the surface plane). Therefore, it is useful to look at the multilayer spectrum (Fig. 3, 500 L), in which all the molecular vibrations should be visible, because the molecules are not restricted to any certain adsorption geometry imposed by the surface. By doing so, a first observation is that the ratio between the CH_2 symmetric and asymmetric stretching modes of the adsorbed glycerol is close to unity, showing both features about the same intensity. Also, in the region corresponding to the skeletal vibrations (1000–1700 cm^{-1}), a characteristic set of peaks with intensity ratios resembling liquid glycerol [54] is seen for the multilayer spectra. It is important to recall here that no free water molecules coadsorbed with glycerol were appreciable in the IRA spectra. They would show up as a broad peak at ~ 1640 cm^{-1} due to the OH bending of water. This peak was observed, though, when glycerol

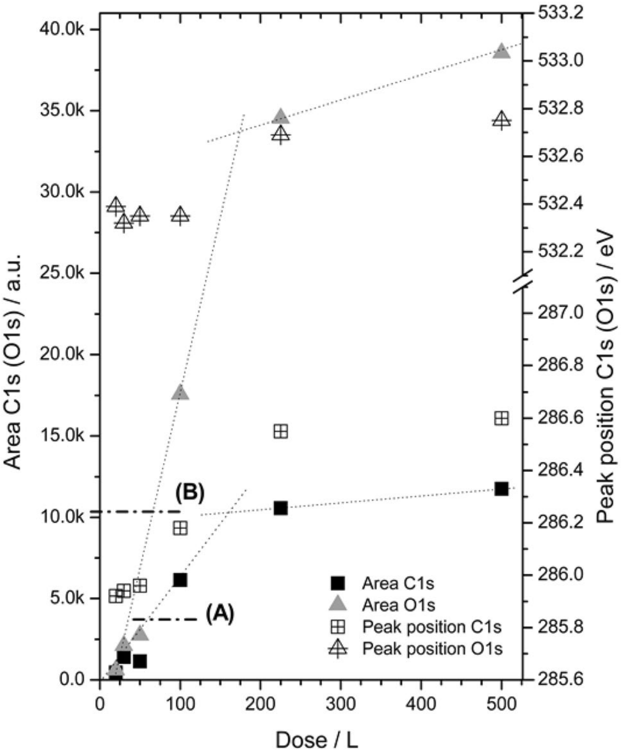

Fig. 2 Integrated areas for the C1s and O1s signals recorded by XPS (left y axis) and their corresponding peak centered positions (right y axis) versus glycerol exposure. **a**, **b** Values of integrated areas for C1s and O1s signals (dashed spectra in Fig. 1a, b), respectively, when 120 L of glycerol is adsorbed at 150 K and further annealed to 260 K

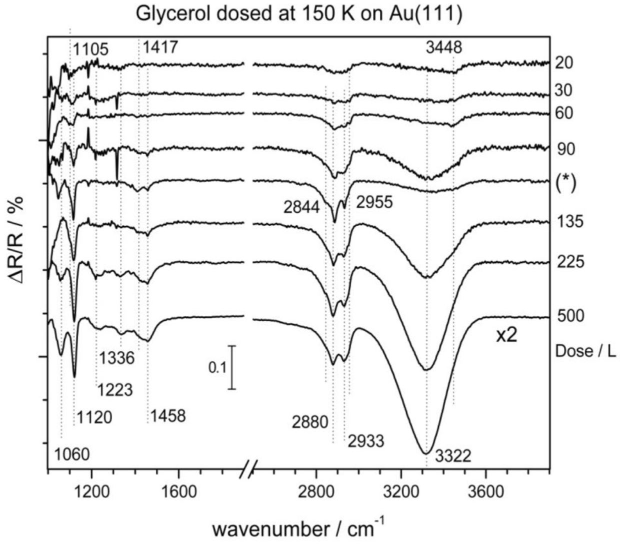

Fig. 3 IRA spectra of glycerol adsorbed on Au(111) at a sample temperature of 150 K. The spectrum indicated with (*) was taken after exposure of 120 L of glycerol at 150 K with further annealing to 260 K (see text)

without a previous purification/distillation was dosed out of the bottle. Furthermore, its disappearance corroborates that the presented experiments are carried out with the purest possible glycerol. Vanderkooi and co-workers [55] studied glycerol–water glasses by IR spectroscopy, and found that only OH stretching and C–OH bending regions are affected by the presence of water and due to hydrogen bonding, and comparison of their spectrum with 0% content of water is excellent proof of the high purity of the glycerol used in this work.

TPD mass spectrometer spectra after adsorption of 100 L of glycerol on Au(111) at 150 K, where several m/z fragments are monitored, are shown in Fig. 4. All observed m/z fragments correspond to molecular glycerol [50, 54] and a characteristic mass spectrometry study of gas phase glycerol and multilayer spectra are shown in SI (Supplementary Information), Fig. S1. It is worth mentioning here that the mass spectrometer used was actually calibrated to be more sensitive to low m/z ratios and therefore the intensity ratios are different than those expected when comparing with the spectrum of glycerol available from NIST [54], and the observation of H_2O and CO accompanying glycerol molecular desorption is explained as extreme decomposition of glycerol on the hot mass spectrometer walls.

There are two desorption peaks observed for m/z = 61 amu (characteristic of glycerol), the first one at ~ 260 K and the second one at 284 K. The one at higher temperature gained in intensity upon increasing exposure until it saturated at about 80 L total dose, while the peak at lower temperature continues growing with larger exposures (spectra not shown). Therefore, the peak at 284 K is assigned to desorption of submonolayer and up to monolayer of adsorbed glycerol and the ~ 260 K peak to desorption of glycerol from the second layer or multilayers. It is worth noting that this differentiation is not as straightforward for this adsorbate as it is for other molecules, due to its intrinsic sticky nature. Furthermore, all detected signals desorbing correspond to molecular glycerol, implying there is no decomposition on Au(111) and therefore no C atoms remain on the surface after each TPD run. This was corroborated by acquiring a C1s XP spectrum after the TPD experiments and finding no signal (data not shown).

The small difference in desorption temperature of monolayer and multilayer glycerol on Au(111) supports the conclusion from the XPS and IRAS data presented above that upon adsorption at low temperature (150 K) multilayer islands start to grow already at submonolayer doses. To isolate the monolayer signals, a new experiment was conducted where ~ 120–140 L of glycerol was dosed at 150 K (at which exposure level already some multilayer is known to condense) and then further annealed to 260 K to desorb all molecules present in second or multilayers. Then, a second IRA spectrum was acquired after cooling the remaining

Table 1 IR assignments (in cm^{-1}) for glycerol adsorbed on clean and oxygen modified Au(111)

Assignments	Gly$^{a}_{(l)}$	Gly$^{b}_{(g)}$	Gly/Au(111)^{c}	Gly/Au(111)^{d}	Gly/O/Au(111)^{e}	Gly/Al$_2$O$_3^{f}$	Gly/Nb$_2$O$_5^{g}$
υOH	3240 br	3665	3440		3260	n/a	n/a
		3625	3320 (tail)	3320 (s)			
$\upsilon_{as}CH_2$	2937	2942	2933	2933	2927	2930	2928
$\upsilon_{s}CH_2$	2880	2890	2880	2880	2877	2876	2872
$\delta_{s/as}CH_2$	1458–1414	1466–1385	1450–1417	1450–1430 br	1400 br	n/a	1458 1413
$\upsilon CC+\delta_{s}CH$	1328	1344		1336		n/a	1326
δCOH	1220	1254–1200		1223	1242–1250	n/a	1208
$\nu CO_{terminal}$	1110	1107	1105	1120	1105	1125–1151	1108 (1140)
$\nu CO_{secondary}$	1040	1054	1050	1060	1057	1083	1045 (1093)

a, b [54]; c–e: this work, c, d: monolayer and multilayer spectra, respectively; f: [62]; g: [64]

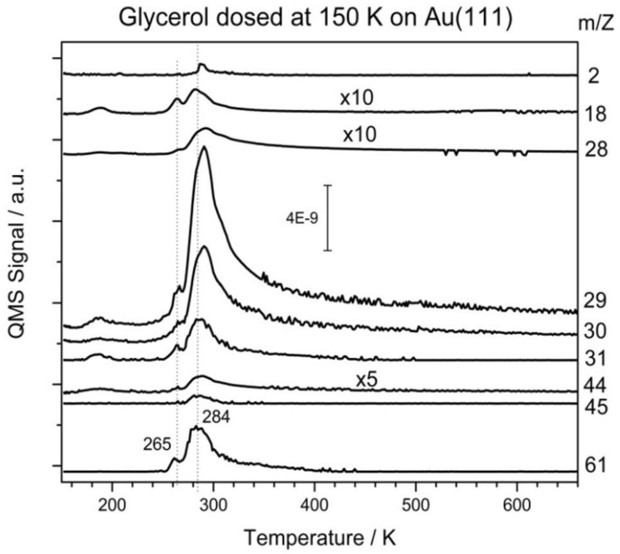

Fig. 4 Glycerol dosed (100 L) at 150 K. TPD heating rate was 1 K/s

monolayer to 150 K. In Fig. 3, the corresponding IRA spectrum is shown and marked as (*). The C1s, O1s and Au4f XP spectra for this same monolayer state are plotted in Fig. 1a–c as dashed lines, and the integrated areas under the C1s and O1s signals are plotted as dashed straight lines marked (A) and (B) in Fig. 2.

The first observation from the experimental results of these ‘monolayer’ IRA and XP spectra is that the exposure level needed to cover the gold surface or, in other words, to avoid forming second layers is in between 60 and 90 Langmuir. In Fig. 3, the corresponding spectrum (*) shows a clear change in conformation of the molecular overlayer besides loosing most of the hydrogen bonding seen at 3320 cm^{-1} which is believed to occur among glycerol molecules of multilayers (intermolecular hydrogen bonding). Kojima et al. [56] studied the liquid–glass transition of glycerol by following the behavior of the O–H stretching vibrational mode with respect to temperature. They observed the evolution of three bands due to the O–H stretches affected by hydrogen bonding, correlated with the density of oligomers present: one centered at 3440 cm^{-1}, assigned to dimeric units and the other two at 3230 and 3340 cm^{-1} corresponding to oligomers with aggregation number larger than two.

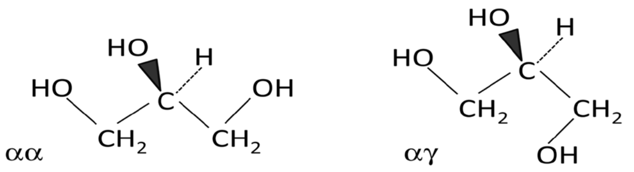

Scheme 1 Glycerol conformer structures (αα and αγ) present in gas or liquid phase

In a recent work by Haadad et al. [57] the 126 possible conformations of 1,2,3-propanetriol (glycerol) were studied by ab initio molecular orbital and DFT calculations in the gas and aqueous phases using multiple levels of theory and basis sets. Their work agrees with previous results from Chelli [58, 59] (DFT): αα and αγ conformations with a slight contribution from γγ (12%) for gas phase and mainly αα for the liquid phase. The αα and αγ structures (drawn in Scheme 1) are accepted to be the stable ones and to be present when glycerol approaches the surface from the gas phase, have two intramolecular hydrogen bonds each: one between the H from one of the terminal OH groups and the central oxygen in OH, the other one between the H of the central OH and the remaining terminal oxygen [60]. In this way, when molecular condensation/crystallization occurs, the hydrogen from a terminal OH and the oxygen which are not participating in any intramolecular hydrogen bond form an intermolecular hydrogen bond [61].

There are no previous IR studies of glycerol adsorbed from the gas phase on any model catalytic surface but only a few works, mainly by Sievers et al. [62–64], which look into the adsorption of glycerol on a variety of oxide powders, proposing a role of acidity-basicity for molecular reactivity on these materials. Even though there is a clear lack of literature data concerning vibrational studies, a good body of work on calculated structures and reactivity of glycerol on metal substrates is available. Liu and Greeley [25] on Pt(111) and Sautet et al. on several other transition metals (Pd, Pt and Rh) [22–24], investigated the decomposition pathways of glycerol either by dehydrogenation or dehydration prior to C–O or C–C cleavage, which ultimately leads to complete decomposition into CO and H_2 on these metals. It is interesting to note that these researchers remark the importance of the intramolecular hydrogen bonds in the reactivity. When approaching the metallic surface, glycerol comes with the two hydrogen bonds previously named, but upon adsorption and depending on which oxygen is thought to interact with the surface, one of said hydrogen bonds is broken, gaining stabilization energy by strongly interacting with the metal atom(s). In the case of glycerol adsorption on Au surfaces, the work by Baltrusaitis et al. [28] shows that the adsorption energy of the molecule is correlated with the d-band center and that, when forming alloys, the presence of the second metal (doping the Au surface) directly affects this parameter. They calculated IR spectra of glycerol adsorbed on clean Au and Au modified by the foreign doping metal, proposing IR spectroscopy as a good tool to follow this effect by monitoring the OH stretching shifts and how this region is affected by the presence of another metal. In the case of interaction of glycerol with Au(111), they considered the molecule approaching the surface in αα configuration (with all OH groups facing the surface) and compared the *ν*OH shifts observed with gas phase glycerol single molecule where no hydrogen bond interactions are taken into account. Nevertheless, the interaction of the oxygen atoms from one terminal and the middle OH groups with Au surface atoms, shifts their vibrations from ca. 3630 cm^{-1} (free OH in the gas phase) to 3460 and 3360 cm^{-1}, respectively. In comparison with the results presented in Fig. 3, the *ν*OH detected upon first doses of glycerol is tentatively assigned to these same vibrations.

3.2 Glycerol Adsorbed on the Oxygen Modified Au(111) Surface

The interaction of O_2 with pristine Au(111) surfaces has been thoroughly studied by other researchers, and the work by Koel et al. [34, 65] and Davis and Goodman [66] are benchmarks on this topic. Most of the past research dealing with activation of O_2 on gold surfaces to obtain either chemisorbed oxygen or gold oxide(s) has been summarized and briefly reviewed by Friend and Madix [67]. In the present work, chemisorbed oxygen atoms on Au(111) were obtained by exposing the surface in front of a hot filament to molecular oxygen. Figure S2 in the Supplementary Information reports the Au4f and O1s XP spectra and the results of O_2 TPD experiments as a function of oxygen dose. For the adsorption of glycerol on O/Au(111) studied here, a relatively low coverage of 0.2 ML (15 L dose) chemisorbed oxygen atoms is chosen [34, 35], on the one hand because the amount of active oxygen species is considered to be low during oxidation reactions on Au, and, on the other hand, to avoid further formation of gold oxide.

IRA spectra taken for increasing doses of glycerol adsorbed on the O/Au(111) surface at 150 K are presented in Fig. 5. Although principally similar vibrational bands compared to adsorption on pristine Au(111) and corresponding to molecular glycerol are observed even at the lowest doses on O/Au(111) (10 L and 20 L, Fig. 5), some differences are encountered that hint a specific interaction between glycerol and O/Au(111). We first mention the shift of the OH stretch vibration to lower wavenumber (3260 cm^{-1} on O/Au(111) compared to 3448 cm^{-1} for small coverage on Au(111) and 3320 cm^{-1} in the condensed phase), which indicates a stronger hydrogen bond interaction of the alcohol groups with the O/Au(111) surface. Together with the hydrogen bonded OH, a broad feature due to δCOH is seen at 1242 cm^{-1}, which was not observed for the glycerol monolayer on pristine Au(111) and is slightly blue-shifted compared to the δCOH vibration in the condensed phase (1223 cm^{-1}, Fig. 3).

By the next doses of glycerol (40–50 L total exposure), the broad feature due to the hydrogen bonded OH develops into a single, broad band with its center moving towards higher wavenumber (3320 cm^{-1}), indicating increasing intermolecular hydrogen bonding due to formation of clusters and/or adsorption of glycerol molecules in the second

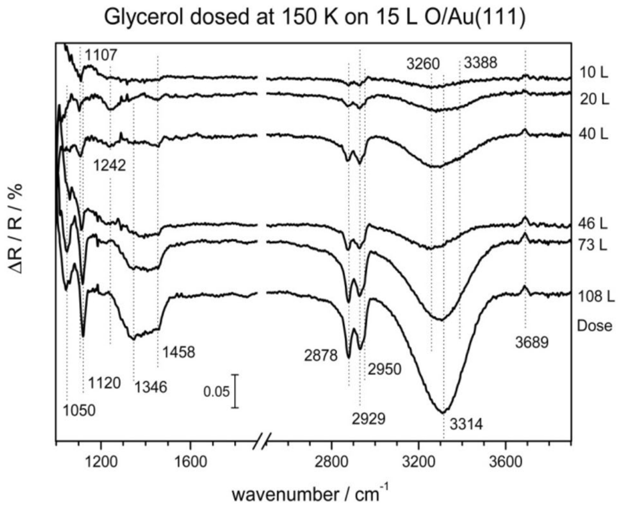

Fig. 5 IRA spectra of glycerol adsorbed on O–Au(111) at 150 K

layer. The band at 1250 cm^{-1} loses some intensity and a new small “positive” band, which was already detectable at lower glycerol doses, fully develops at 3686 cm^{-1}, and is most likely due to (non-hydrogen bonded) Au–OH species. Observing a positive band indicates that those species were present on the surface before the background IR spectrum was acquired. In other words, this observation tells that at least some of the chemisorbed oxygen is actually in the form of OH and that glycerol interacts with some OH species upon adsorption at 150 K. The remaining vibrations due to CH and CH$_2$ groups (2850–3000 cm^{-1}) are not strongly affected by the presence of oxygen (or OH) as they appear at the same wavenumber as seen for the pristine Au(111) surface, though with slightly different intensity ratio, which could be indicative of a slight change in the adsorption geometry. In this respect it is noticeable that the 2927 cm^{-1} band (ν_{as}CH$_2$) has a higher intensity than the 2877 cm^{-1} band (ν_sCH$_2$), unlike for adsorption of glycerol on the pristine Au(111) surface. This could in principle be explained by the interaction of the middle OH group with the O–Au groups, which tilts both terminal CH$_2$ groups in a way that favors the enhanced observation of their asymmetric stretch. For the C–O stretches, the 1107 cm^{-1} band, due to the νC–O of the terminal alcohol groups, is at the same position as for the adsorption on the pristine surface. The remaining bands in the region are not well resolved and the band at 1060–1050 cm^{-1} due to νC–O of the central alcohol group does not fully develop until higher glycerol doses, when most probably the effect of chemisorbed oxygen is not accountable anymore. Upon adsorption of 100 L already the appearance of some second or multilayers is seen with most of the observed vibrations corresponding to those of liquid glycerol [54].

To further investigate the interaction and reactivity of glycerol on O/Au(111), a TPD experiment was performed for submonolayer coverage (30 L total dose) of glycerol on 0.2 ML O/Au(111). As seen in Fig. 6, desorption of molecular glycerol (61 amu) is completely absent, meaning that all adsorbed glycerol molecules have been partially or completely oxidized during the TPD run. The oxidation products include aldehyde and carboxylic acid groups as identified by the major detected fragments with 29 amu (HCO), 30 amu (H$_2$CO) and 44 amu (CO$_2$), in addition to codesorbing water (18 amu). The onset of glycerol oxidation/decomposition appears already at 210 K and has a first maximum at 254 K, with noticeable evolution of the 29 amu and 30 amu fragments (HCO and H$_2$CO fragments) together with water, but comparably little CO$_2$. This indicates formation and desorption of aldehyde species. A second ‘wave’ of these fragments desorbs at 293 K, this time with a large contribution of CO$_2$. This is assigned to the evolution of products containing an acid group (COOH), such as tartronic acid (with appreciable amounts of m/z = 29, 30, 44 and 45 amu in its fragmentation pattern [54]), which would imply that both terminal OH groups of glycerol were oxidized, or simply formic acid, which requires cleavage of the C–C bond in the adsorbed glycerol molecule. In addition, complete oxidation to water and CO$_2$ might also occur. Barely detectable but quite noticeable is the evolution of a fragment with m/z = 31 amu with two distinct peaks at 209 and 266 K. This points to formation and desorption of dihydroxyacetone (DHA), which presents maximum intensity in its fragmentation pattern for this fragment. Finally, it has to be pointed out that no hydrogen (2 amu) and hardly any remaining oxygen (32 amu) was detected in this TPD experiment, showing that all chemisorbed oxygen was consumed in the oxidation reactions and hydrogen stemming from dehydrogenation of glycerol desorbed as water. Again, C1s and O1s XP spectra were acquired after the TPD experiments finding no signal for neither of them (data not shown).

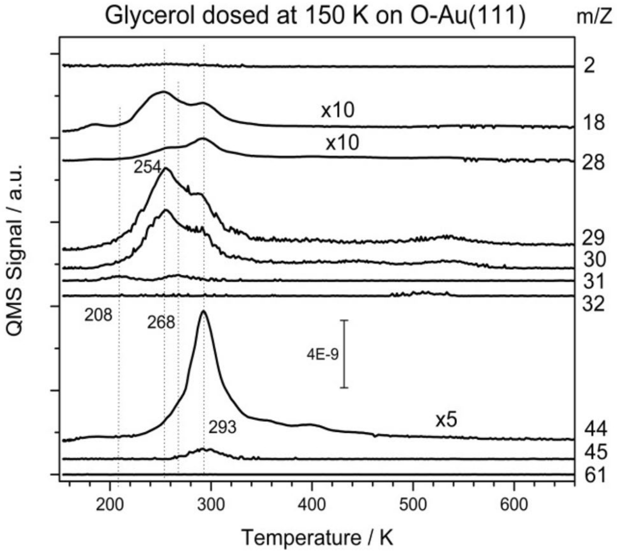

Fig. 6 TPD after dosing glycerol (30 L) at 150 K on the oxygen pre-activated (15 L) Au(111) surface. Heating rate was 1 K/s

Even though desorption of oxidation products from the surface is a clear indication of the reaction between the chemisorbed oxygen atoms (and hydroxyl groups) with glycerol molecules, gaining clear-cut information about possible intermediates for this reaction is not straightforward using the TPD technique. To gain more insight, additional spectroscopic experiments were performed, where O/Au(111) was exposed to glycerol at 150 K and then annealed to specific temperatures, as shown in the next figures. First, Fig. 7a, b shows C1s and O1s XP spectra for the annealing experiment, respectively. For comparison purposes, the corresponding spectra for O/Au(111) taken prior to glycerol exposure are plotted at the bottom of the figure.

Before glycerol adsorption, the O1s signal corresponding to O$_{ads}$ on Au(111) at 529.3 eV is clearly appreciable. This

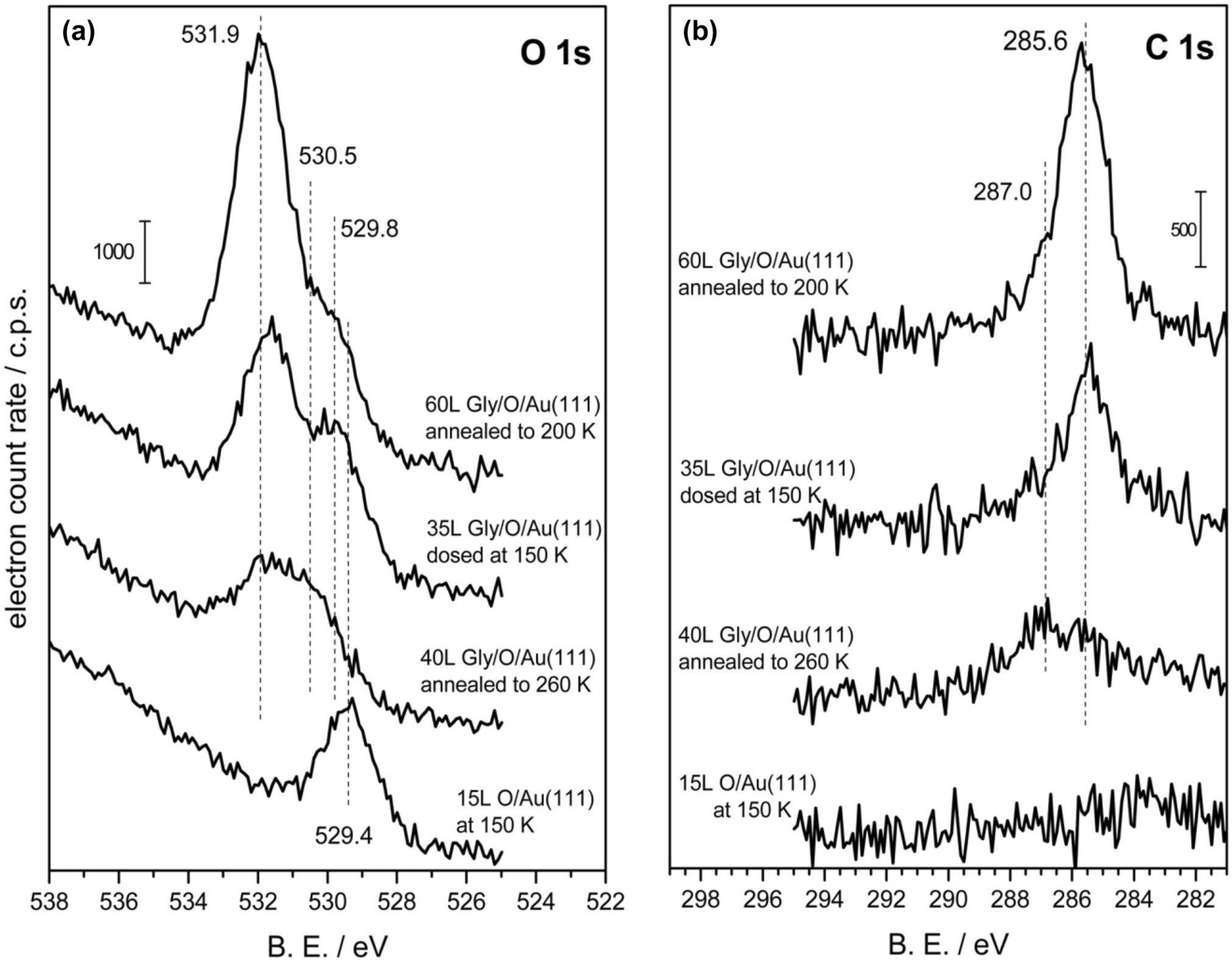

Fig. 7 XP spectra for C1s and O1s region before and after TPD of Gly/O/Au (see text)

same signal is still observable after adsorbing glycerol, but shifted by 0.4 eV to higher binding energy (529.7 eV) due to hydrogen bond interaction with adsorbed glycerol. Correspondingly, the C1s and O1s XP signals of glycerol on O/Au(111) are shifted to lower binding energy compared to the case of adsorption on pristine Au(111), by 0.3 eV and 0.4 eV, respectively. This effect of binding energy shifts due to hydrogen bond interactions has been studied in detail by Kerber et al. [68], and in the case presented here is due to interaction of the alcohol groups (either terminal or central) with chemisorbed oxygen atoms:

$$RCH_2{-}O{-}H \cdots O{-}Au \rightarrow RCH_2{-}O \cdots H{-}O{-}Au$$

The result of heating the overlayer of coadsorbed glycerol and oxygen is shown for temperatures of 200 K and 260 K. These values correspond to the temperature range where some of the intermediates for the oxidation products are expected to be present according to the TPD results (Fig. 6). Upon heating to 200 K, spectral fitting of the O1s spectrum reveals, in addition to $\mathbf{O}_{\mathbf{ads}}$ and the C–**O**H species, the presence of a new O1s peak at 530.7 eV (Fig. 7b), which can be assigned to carbonyl (C=**O**) bonds [32, 33, 41]. The carbonyl signal is still observed upon further heating to 260 K (Fig. 7b), thus suggesting that C=O formation is an integral part of the oxidation of glycerol. This is further confirmed by the corresponding C1s spectra shown in Fig. 7a. In addition to the **C**–OH signal, a new C1s signal with a binding energy of 287.0 eV, assigned to the formation of **C**=O groups, can be clearly observed in the heating experiments. A quantitative treatment of this data (by using XPSPeak 4.1) was performed and is shown in the Supporting Information (Fig. S3). Certainly, what cannot be inferred from these results is whether only one, two or all the C–OH moieties transform into carbonyl groups. This aspect notwithstanding, it is apparent that the pathway of glycerol decomposition proceeds through dehydrogenation of the alcohol groups in the presence of adsorbed oxygen (and adsorbed OH), therefore releasing water as seen in TPD.

Finally, the heating experiment was repeated and the species present on the surface and evolving with temperature monitored using infrared spectroscopy, as shown in Fig. 8, starting with the IRA spectrum of 40 L glycerol dosed onto O/Au(111) at 150 K (bottom spectrum). The other spectra are the difference spectra between the spectrum corresponding to the temperature up to which the sample was heated and the one corresponding to the state of the overlayer at the previous temperature. In this way, small features, which might be due to the intermediates, can be more easily discerned from the overall features of the overlayer (the corresponding set of spectra where the results are plotted using the same background spectrum before adsorption of glycerol are shown in the Supplementary Information, Fig. S4).

The spectrum taken after adsorption of 40 L glycerol on O/Au(111) at 150 K is similar to the one for 46 L glycerol presented and discussed above (Fig. 5). Upon heating to 180 K, a very small but already detectable feature at 1714 cm^{-1} emerged, which indicates the appearance of the C=O stretching signal due to oxidation of some of the OH groups of the adsorbed glycerol. The positive peaks in the CH stretching region can most likely be assigned to the disappearance of some H (by dehydrogenation of CH and CH$_2$ moieties to form C=O), rather than to reordering of the overlayer, because—as pointed out in what follows—this trend perceptibly increases with heating.

When the overlayer is warmed up to 230 K, the 230/180 K difference spectrum clearly shows the vibration corresponding to C=O at 1734 cm^{-1}, accompanied by positive (meaning disappearance) peaks in the CH stretching region, together with the small broad feature seen at 1242 cm^{-1}. The vibration at 1110 cm^{-1} (seen positive, disappearing) should correspond to any of the two terminal OH groups, but it has to be kept in mind—in the first place—that the 1050–1060 cm^{-1} peak corresponding to the secondary alcohol group was not seen when dosing glycerol on the oxygen modified surface. Another explanation for not observing the C–OH stretch is that some C–C cleavage occurred and the fragments adsorbed consist of only C2 species, like glycol derivatives. Thirdly, the appearance of features at 1336 and 1383 cm^{-1} are perfectly discerned. These two last features could correspond to some CH bends detectable due to an adsorption geometry which favors the observation of these modes. A good possibility is these features are due to carboxylate species featuring OCO stretch signatures due to further oxidation of the alcohol moieties, but the XP spectra should detect clearly those features at binding energies higher than 287 eV for the C1s signals, which is not the case. The only possibility would be if the second oxygen is inserted as an alcoxy bond on either one or both terminal C–OH groups. In this way the C1s signal will show up as a dialcoxy (O–C–O) resembling that for a carbonyl (C=O) bond, when analyzing its C1s signal position. This effect has been seen for adsorption and further decomposition of ethylene glycol (H$_2$C(OH)–C(OH)H$_2$) on CeO$_2$(111) films [46]. Glycerol interaction with niobia surfaces presents formation of a bridge bonded alcoxy through one of the terminal COH groups interacting with surface hydroxyls [64].

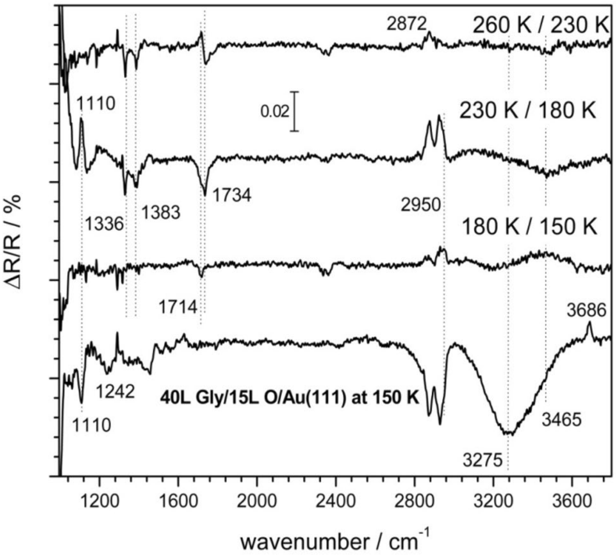

Fig. 8 IRAS after dosing 40 L of glycerol on O–Au(111) at 150 K with further annealing to the indicated temperatures (upper traces are difference spectra—see text)

By heating the overlayer once more, to 260 K (this is comparable to what is seen then in XPS, Fig. 7), the features corresponding to the C=O shift somewhat and decrease in intensity while, at the same time, the doublet at 1336 and 1386 cm^{-1} becomes stronger. No new incremental changes are observable in the CH stretching region between 230 and 260 K, besides a small positive peak centered at approx. 2872 cm^{-1}, indicating there is probably no more appreciable dehydrogenation of the molecule or adsorbed species.

A complete pathway for the decomposition reaction of glycerol on the oxygen-covered Au surface cannot be straightforwardly presented, due to the many different reaction possibilities offered by the three alcohol moieties in the molecule. Nevertheless, it is important to remark from the present results that the Au–OH species detected right upon adsorption of glycerol on the oxygen-covered Au surface are not only an impurity formed during the oxygen exposure, but might be actively involved in the oxidation of glycerol on the surface. Some researchers proposed that the presence of water might strongly affect the reactivity of flat, otherwise unreactive Au surfaces, which is explained by the formation of surface hydroxyls. But these hydroxyls are not stable species/intermediates and their presence and effect on the partial oxidation reaction mechanism can only by inferred indirectly from the experiments. Friend's research group has proposed that transient hydroxyls make Au good for partial oxidation reactions, by studying the interaction of water with a O/Au(111) surface [69]. The main proof comes from isotopic exchange experiments where the distribution of products seems to indicate the only possibility is the presence and further reactivity of Au–OH species during reaction. In the same trend of thought is found the work by Neurock and Davis [70], where also the presence of Au–OH has been recalled as the pertinent oxidative species for glycerol/ethanol partial and further total oxidation. From the present results it is clear that the Au–OH groups contribute to the initial adsorption of glycerol at 150 K by establishing a hydrogen bond between the oxygen of the alcohol groups with the hydrogen atom of Au–OH. A slight temperature rise of only 30 K (from 150 to 180 K) is sufficient to activate the already modified C–OH group facilitating its dehydrogenation and oxidation to a carbonyl group (C=O).

Regarding the different products obtained by partially oxidation of glycerol during heating, a simple scheme with a variety of possibilities is presented in Scheme 2. The two aldehyde products are obtained by dehydrogenation of either one terminal OH or the central OH are dihydroxyacetone (DHA) or glyceraldehyde, respectively. Partial oxidation of the central C–OH is actively sought and it has been demonstrated that the alloying of Pt with Bi and reacting glycerol with O_2 in acidic media greatly increases selectivity toward DHA [71]. On the other hand, deeper oxidation of glycerol on Pt or Pd catalysts in basic media yields mainly products implying oxidation of the primary C–OH groups, namely glyceric acid or tartronic acid [72]. Even though the electrooxidation of glycerol on Pt films is not directly comparable to the partial oxidation reaction studied in the present work, still the results from the group of Behm, regarding possible intermediates present on the surface of the working electrode by IR spectroscopy [73], could provide some information about the intermediates present on glycerol/O–Au(111). In that work, the authors detected some type of acetyl species appearing at intermediate potentials during glycerol electrooxidation, with a signature in IR at 1640 cm^{-1} assigned to the C=O stretching vibration of an acyl carbonyl group from a species adsorbed through the C atom. This species was explained to come from oxidation of the terminal OH groups and named “glyceroyl” due to their resemblance to glyceraldehyde (even though probably both H atoms from CH_2 still prevail on the C atom). When comparing with the feature observed during adsorption of glyceraldehydes on the same Pt films, they found another feature at 1720 cm^{-1} which they refrained to explain further. Nevertheless, both Pd and Pt catalysts showing high activity for oxidation of glycerol to glyceric acid present the problem of high deactivation rate due to coke formation (easy cleavage of C–C bonds, beside dehydrogenation) and fast poisoning by CO adsorption on active sites being extremely stable.

The oxidation of glycerol by Au catalysts has been thoroughly studied by the group of Pratti, and very recently reviewed by this same group [15]. On these catalysts, high activity and selectivity towards glyceric acid was obtained in basic conditions. The need for basic conditions could be overcome by combining Au with a more reactive metal like

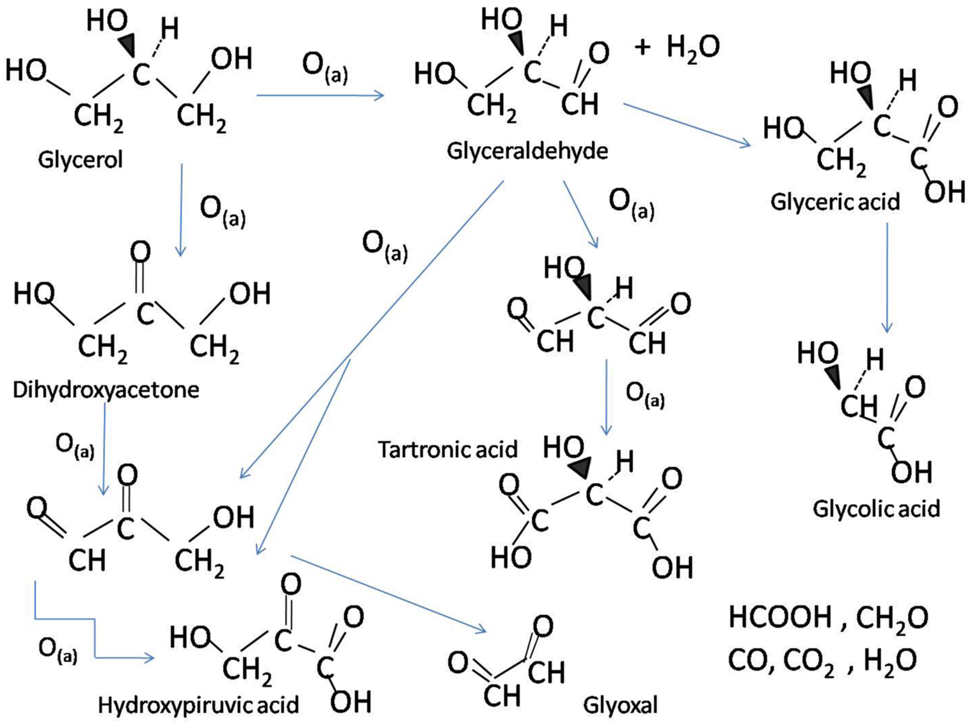

Scheme 2 Possible reaction pathways for glycerol oxidation and decomposition on O/Au(111)

Pd or Pt as a bimetallic system, which has also the effect of lowering the deactivation rate by diluting the more active metal with Au atoms. Camara et al. [74] studied the electrooxidation reaction of glycerol on polycrystalline Au by IR spectroscopy and they found the pathway via glyceraldehyde → glycerate as the main one for partial oxidation, being able to further oxidize the glycerate species (1307 cm^{-1}) to hydroxypyruvate species (1355 cm^{-1}) or further desorb as glyceric acid. They also observed production of CO_2 by total oxidation and C–C cleavage.

Summarizing all conclusions from the reactivity data and spectroscopic techniques used in the present work, the most plausible mechanism for decomposition of glycerol on Au surfaces in the presence of chemisorbed oxygen, and under the conditions studied, is drawn in Scheme 2.

We can tentatively explain the reactivity of glycerol adsorbed on the O/Au(111) surface by the initial interaction of either the terminal or central C–OH groups with O–Au or HO–Au by hydrogen bond interaction at low temperature (150 K). Upon heating, the first oxidation step leads to aldehyde or ketonic intermediates as detected by XPS and IRAS. These intermediates are further oxidized to glycerate species or, if C–C cleavage is possible, oxidized C2 intermediates, which are easy to decompose on the Au surface leading to CO_2 and H_2O.

4 Conclusions

Glycerol interacts weakly with the Au(111) surface, showing non activated adsorption at 150 K and its complete molecular desorption below room temperature in TPD experiments. Only weak interactions between oxygen atoms from the alcohol groups and Au atoms are responsible for its binding and possibly affect the intra and intermolecular hydrogen bonding within the monolayer.

The presence of oxygen atoms and hydroxyls chemisorbed on Au(111) prior to glycerol adsorption readily activates the molecule by modifying the hydrogen bonding interaction and facilitating C–H and CO–H cleavage to form carbonyl C=O containing intermediates, indicating partial oxidation. These intermediates are identified by the νCO at 1714–1740 cm^{-1} in IRAS and a C1s peak at 287 eV in XPS. Further oxidation of these intermediates toward C3 and C2 carboxylic acids is confirmed by detection of νOCO carboxylate features (1336–1383 cm^{-1}) and desorption of characteristic fragments during the temperature ramp in TPD, up to total oxidation to CO_2 and H_2O. The observed participation of Au–OH groups, in addition to chemisorbed oxygen, in the activation of glycerol indicates the importance of ambient reactivity in the presence of water or humid conditions for rendering an otherwise unreactive metal potentially active toward partial selective oxidation.

Acknowledgements FCC greatly acknowledges support by the Alexander von Humboldt Foundation through a Georg Foster Postdoctoral fellowship.

Compliance with Ethical Standards

Conflict of interest The authors declare that they have no conflict of interest.

References

1. Centi G, van Santen RA (2007) Catalysis for renewables. From feedstock to energy production. Wiley-VGH Verlag, Weinheim
2. Ragauskas AJ (2006) The path forward for biofuels and biomaterials. Science 311(5760):484–489
3. Dimitratos N, Lopez-Sanchez JA, Hutchings GJ (2009) Green catalysis with alternative feedstocks. Top Catal 52:258–268
4. Huber GW, Dumesic JA (2006) An overview of aqueous-phase catalytic processes for production of hydrogen and alkanes in a biorefinery. Catal Today 111:119–132
5. Climent M, Corma A, Iborra S (2014) Production of liquid alkanes by aqueous-phase processing of biomass-derived carbohydrates. Green Chem 16:516–547
6. Singh SP, Singh D (2010) Biodiesel production through the use of different sources and characterizationof oils and their esters as the substitute of diesel: a review. Renew Sustain Energy Rev 14:200–216
7. Huang H, Long S, Singh V (2015) Ultra oil-producing. AOCS INFORM 26(5):278–282
8. D'Angelo S, Dall'Ara A, Mondelli C, Pérez-Ramírez J, Papadokonstantakis S (2018) Techno-economic analysis of a glycerol biorefinery. ACS Sustain Chem Eng 6:16563–16572
9. Pagliaro M, Ciriminna R, Kimura H, Rossi M, Della Pina C (2007) From glycerol to value-added products. Angew Chem Int Ed 46:4434–4440
10. Dasari M, Kiatsimkul P, Sutterlin W, Suppes G (2005) Low-pressure hydrogenolysis of glycerol to propylene glycol. Appl Catal A 281:225–231
11. Haider M, Dummer N, Knight D, Jenkins R, Howard M, Moulijn J, Taylor S, Hutchings G (2015) Efficient green methanol synthesis from glycerol. Nat Chem 7:1028–1032
12. Dodekatos G, Schünemann S, Tüysüz H (2018) Recent advances in thermo-, photo-, and electrocatalytic glycerol oxidation. ACS Catal 8:6301–6333
13. Prati L, Spontoni P, Gaiassi A (2009) From renewable to fine chemicals through selective oxidation: the case of glycerol. Top Catal 52:288–296
14. Davis SE, Matthew A, Idea S, Davis RJ (2013) Selective oxidation of alcohols and aldehydes over supported metal nanoparticles. Green Chem 15:17–45
15. Cattaneo S, Stucchi M, Villa A, Prati L (2019) Gold catalysts for the selective oxidation of biomass-derived products. ChemCatChem 11:309–323
16. Pembere AM, Luo Z (2017) Jones oxidation of glycerol catalysed by small gold clusters. Phys Chem Chem Phys 19:6620–6625
17. Brett GL, He Q, Hammond C, Miedziak PJ, Dimitratos N, Sankar M, Andrew A, Herzing AA, Conte M, Lopez-Sanchez JA, Kiely CJ, Knight DW, Taylor SH, Hutchings GJ (2011) Selective oxidation of glycerol by highly active bimetallic catalysts at ambient temperature under base-free conditions. Angew Chem Int Ed 50:10136–10139
18. Rodrigues EG, Carabineiro C, Chen X, Delgado JJ, Figueiredo JL, Pereira MFR, Orfao JJM (2011) Selective oxidation of glycerol

catalyzed by Rh/activated carbon: importance of support surface chemistry. Catal Lett 141:420–431

19. Villa A, Manzoli M, Vindigni F, Chinchilla LE, Botton GA, Prati L (2017) Diols production from glycerol over Pt-based catalysts: on the role played by the acid sites of the support. Catal Lett 147(5):1–11
20. Jouve A, Stucchi M, Barlocco I, Evangelisti C, Somodic F, Villa A, Prati L (2018) Carbon-supported Au nanoparticles: catalytic activity ruled out by carbon support. Topics Catal 61:1928–1938
21. Varghese JJ, Cao L, Robertson C, Yang Y, Gladden LF, Lapkin LA, Mushrif SH (2019) Synergistic contribution of the acidic metal oxide–metal coupleand solvent environment in the selective hydrogenolysis of glycerol: a combined experimental and computational study using ReOx–Ir as the catalyst. ACS Catal 9(1):485–503
22. Auneau F, Michel C, Delbecq F, Pinel C, Sautet P (2011) Unravelling the mechanism of glycerol hydrogenolysis over rhodium catalyst through combined experimental–theoretical investigations. Chem Eur J 17:14288–14299
23. Coll D, Delbecq F, Aray Y, Sautet P (2011) Stability of intermediates in the glycerol hydrogenolysis on transition metal catalysts from first principles. Phys Chem Chem Phys 13:1448–1456
24. Sautet M (2011) C-H versus O-H Bond dissociation for alcohols on a Rh(111) surface. A strong assistance from hydrogen bonded neighbors. ACS Catal 1(10):1430–1440
25. Liu B, Greeley J (2011) Decomposition pathways of glycerol via C-H, O-H, and C-C bond scission on Pt(111): a DFT Study. J Phys Chem C 115:19702–19709
26. Shan N, Liu B (2018) Elucidating molecular interactions in glycerol adsorption at the metal-water interface DFT. Langmuir 35(14):4791–4805
27. Cortese R, Schimmenti R, Armata N, Ferrante F, Prestianni A, Duca D, Murzin DY (2015) Investigation of polyol adsorption on Ru, Pd, and Re using vdW density functional. J Phys Chem C 119:17182–17192
28. Baltrusaitis J, Valter M, Hellman A (2016) Geometry and electronic properties of glycerol adsorbed on bare and transition-metal surface-alloyed Au(111): a density functional theory study. J Phys Chem C 120(3):1749–1757
29. Meyer R, Lemire C, Shaikhutdinov ShK, Freund H-J (2004) Surface chemistry by gold. Gold Bull 37(1–2):72–124
30. Carabineiro SAC, Nieuwenhuys BE (2009) Adsorption of small molecules on Au. Gold Bull 42(4):288–301
31. Jenniskens HG, Dorlandt PWF, Kadodwala MF, Kleyn AW (1996) The adsorption of methanol on Ag(111) studied with TDS and XPS. Surf Sci 357–358:624–628
32. Bowker M, Madix RJ (1982) XPS, UPS and thermal desorption studies of alcohol adsorption on Cu(110). II. Higher alcohols. Surf Sci 116:549–572
33. Sexton BA, Hughes AE (1984) A comparison of weak molecular adsorption of organic molecules on clean copper and platinum surfaces. Surf Sci 140:227–248
34. Lazaga MA, Wickham DT, Parker DH, Kastanas GN, Koel BE (1983) Reactivity of oxygen adatoms on the Au(111) surface. ACS Symp Ser 523:90–109
35. Gong J, Flaherty DW, Ojifinni RA, White JM, Buddie Mullins C (2008) Surface chemistry of methanol on clean and atomic oxygen pre-covered Au(111). J Phys Chem C 112(14):5501–5509
36. Outka DA, Madix RJ (1987) Broensted basicity of atomic oxygen on the gold(110) surface: reactions with methanol, acetylene, water, and ethylene. J Am Chem Soc 109(6):1708–1714
37. Vinod CP, Niemantsverdriet JW, Nieuwenhuys BE (2005) Decomposition of methanol on Au(310). Phys Chem Chem Phys 7:1824–1829
38. Attard GA, Chibane HD, Parsons ER (1989) The adsorption and decomposition of methanol on Pt(110). Surf Sci 224:311–326
39. Sexton BA, Rendulic KD, Huges AE (1982) Decomposition pathways of C1-C4 alcohols adsorbed on platinum (111). Surf Sci 121:181–198
40. Chen JJ, Jiang Z-C, Zhou Y, Chakraborty BR, Winograd N (1995) Spectroscopic studies of methanol decomposition on Pd(111). Surf Sci 328:248–262
41. Borasio M, Rodríguez de la Fuente O, Rupprechter G, Freund H-J (2005) In situ studies of methanol decomposition and oxidation on Pd(111) by PM-IRAS and XPS Spectroscopy. J Phys Chem B 109(38):17791–17794
42. Skoplyak O, Barteau MA, Chen JG (2006) Reforming of oxygenates for H2 production: correlating reactivity of ethylene glycol and ethanol on Pt(111) and Ni/Pt(111) with surface d-band center. J Phys Chem B 110(4):1686–1694
43. Stottlemyer AL, Rren H, Chen JG (2009) Reactions of MeOH and EG on Ni-Pt: bridging the materials gap between single crystal and polycrystalline bimetallic surfaces. Surf Sci 603:2630–2638
44. Jansen MMM, Nieuwenhuys BE, Niemantsverdriet H (2009) Chemistry of ethylene glycol on a Rh(100) single-crystal surface. ChemSusChem 2:883–886
45. Griffin MB, Jorgensen EL, Medlin JW (2010) The adsorption and reaction of ethylene glycol and 1,2-propanediol on Pd(111): a TPD and HREELS study. Surf Sci 604:1558–1564
46. ChenT-L Mullins DR (2011) Ethylene glycol adsorption and reaction over CeOx(111) thin films. J Phys Chem C 115(28):13725–13733
47. Li Z, Kay BD, Dohnálek Z (2013) Dehydration and dehydrogenation of ethylene glycol on rutile TiO_2(110). Phys Chem Chem Phys 15:12180–12186
48. Chen L, Li Z, Scott Smith R, Kay BD, Dohnálek Z (2014) Conversion of 1,2-propylene glycol on Rutile TiO_2(110). J Phys Chem C 118(28):15339–15347
49. Chen L, Li Z, Scott Smith R, Kay BD, Dohnálek Z (2014) Conversion of 1,3-propylene glycol on rutile TiO_2(110). J Phys Chem C 118(40):23181–23188
50. Skoplyak O, Barteau MA, Chen JG (2008) Enhancing H_2 and CO production from glycerol using bimetallic surfaces. ChemSusChem 1(6):524–526
51. Zehmner DM, Wendelken JF (1977) Anomalous Au(111) surfaces studies by LEED, AES, and oxygen chemisorptions (ORNL). In: 7th international vaccum congress and 3rd international conference on solid surfaces, Vienna, Austria, 12 Sep 1977
52. McGuirk GM, Shin H, Caragiu M, Ash S, Bandyopadhayay PK, Prince RH, Diehl RD (2013) Au(111) surface structures induced by adsorption. LEED I(E) analysis of (1 × 1) and (5 × 5) Au(111)–S phases. Surf Sci 610:42–47
53. Min BK, Deng X, Pinnaduwage D, Schalek R, Friend CM (2005) Oxygen-induced restructuring with release of gold atoms from Au(111). Phys Rev B 72:121410(R)
54. NIST Chemistry webbook (Glycerol, CAS: 56-81-5) https://webbook.nist.gov/cgi/cbook.cgi?ID=56-81-5&Units=SI; (Tartronic acid, CAS: 80-69-3) https://webbook.nist.gov/cgi/cbook.cgi?ID=C80693&Mask=200#Mass-Spec
55. Zelent B, Nucci NV, Vanderkooi JM (2004) Liquid and ice water and glycerol-water glasses compared by IR spectroscopy. J Phys Chem A 108:11141–11150
56. Kojima S (1993) Anomalous behavior of the OH stretching vibrational mode in the liquid-glass transition of glycerol. J Mol Struct 294:193–196
57. Callam CS, Singer SJ, Lowary TL, Hadad CM (2001) Computational analysis of the potential energy surfaces of glycerol in the gas and aqueous phases: effects of level of theory, basis set, and solvation on strongly intramolecularly hydrogen-bonded systems. J Am Chem Soc 123:11743–11754

58. Chelli R, Gervasio FL, Gellini G, Procacci P, Cardini G, Schettino V (2000) Density functional calculations of structural and vibrational properties of glycerol. J Phys Chem A 104:5351–5357
59. Chelli R, Gervasio FL, Gellini G, Procacci P, Cardini G, Schettino V (2000) Conformational distribution of gas-phase glycerol. J Phys Chem A 104(47):11220–11222
60. Jeon K-H, Byun B-J, Kang Y-K (2012) Conformational preferences of glycerol in the gas phase and in water. Bull Korean Chem Soc 33(3):917–924
61. Kusukawa T, Niwa G, Sasaski T, Oosawa R, Himeno W, Kato M (2013) Observation of a hydrogen-bonded 3D structure of crystalline glycerol. Bull Chem Soc Jpn 86(3):351–353
62. Copeland JR, Shi X-R, Sholl DS, Sievers C (2013) Surface interactions of C2 and C3 polyols with α-Al_2O_3 and the role of co-adsorbed water. Langmuir 29:581–593
63. Copeland JR, Santillan IA, McNew Schimming S, Ewbank JL, Sievers C (2013) Surface interaction of glycerol with acidic and basic metal oxides. J Phys Chem C 117:21413–21425
64. Foo GS, Wei D, Sholl DS, Sievers C (2014) Role of Lewis and Broensted acid sites in the dehydration of glycerol over Niobia. ACS Catal 4:3180–3192
65. Saliba N, Parker DH, Koel BE (1998) Adsorption of oxygen on Au(111) by exposure to ozone. Surf Sci 410(2):270–282
66. Davis KA, Goodman DW (2000) Propene adsorption on clean and oxygen-covered Au(111) and Au(100) surfaces. J Phys Chem B 104:8557
67. Montemore MM, van Spronsen MA, Madix RJ, Friend CM (2018) O_2 Activation by metal surfaces: implications for bonding and reactivity on heterogeneous catalysts. Chem Rev 118(5):2816–2862
68. Kerber SJ, Bruckner JJ, Wozniak K, Seal S, Hardcastle S, Barr TL (1996) The nature of hydrogen in X-ray photoelectron spectroscopy: general patterns from hydroxides to hydrogen bonding. J Vac Sci Technol A 14(3):1314–1320
69. Quiller RG, Baker TA, Deng X, Colling ME, Min BK, Friend CM (2008) Transient hydroxyl formation from water on oxygen-covered Au(111). J Chem Phys 129:0647029
70. Zope BN, Hibbitts DD, Neurock M, Davis RJ (2010) Reactivity of the gold/water interface during selective oxidation catalysis. Science 330:74–78
71. Gallezot P (1997) Selective oxidation with air on metal catalysts. Catal Today 37:405–418
72. Garcia R, Besson M, Gallezot P (1995) Chemoselective catalytic oxidation of glycerol with air on platinum metals. Appl Catal A 127:165–176
73. Schnaidt J, Heinen M, Denot D, Jusys Z, Behm RJ (2011) Electrooxidation of glycerol studied by combined in situ IR spectroscopyand online mass spectrometry under continuous flow conditions. J Electroanal Chem 661:250–264
74. Jeffery DZ, Camara GA (2010) The formation of carbon dioxide during glycerol electrooxidation in alkaline media: first spectroscopic evidences. Electrochem Commun 12:1129–1132